VIIRS captures phytoplankton vertical migration in the NE Gulf of Mexico

Lin Qi[a,b,*], Chuanmin Hu[c], Brian B. Barnes[c], Zhongping Lee[d]

[a] State Key Laboratory of Marine Environmental Science, Xiamen University, Xiamen, China
[b] State Key Laboratory of Lake Science and Environment, Nanjing Institute of Geography and Limnology, Chinese Academy of Sciences, Nanjing, China
[c] College of Marine Science, University of South Florida, St. Petersburg, FL, USA
[d] School for the Environment, University of Massachusetts Boston, Boston, MA, USA

ARTICLE INFO

ABSTRACT

In summer 2014, a toxic *Karenia brevis* bloom (red tide) occurred in the NE Gulf of Mexico, during which vertical migration of *K. brevis* has been observed from glider measurements. The current study shows that satellite observations from the Visible Infrared Imaging Radiometer Suite (VIIRS) can capture changes in surface reflectance and chlorophyll concentration occurring within 2 h, which may be attributed this *K. brevis* vertical migration. The argument is supported by earlier glider measurements in the same bloom, by the dramatic changes in the VIIRS-derived surface chlorophyll, and by the consistency between the short-term reflectance changes and those reported earlier from field-measured *K. brevis* vertical migration. Estimates using the quasi-analytical algorithm also indicate significant increases in both total absorption coefficient and backscattering coefficient in two hours. The two observations in a day from a single polar-orbiting satellite sensor are thus shown to be able to infer phytoplankton vertical movement within a short timeframe, a phenomenon difficult to capture with other sensors as each sensor can provide at most one observation per day, and cross-sensor inconsistency may make interpretation of merged-sensor data difficult. These findings strongly support geostationary satellite missions to study short-term bloom dynamics.

© 2017 Elsevier B.V. All rights reserved.

1. Background

Karenia brevis, a toxic algae responsible for most harmful algal blooms (red tides) in the Gulf of Mexico (GOM), is known to migrate vertically with diel cycles to maximize its use of light and nutrients. This phenomenon has been observed and studied numerous times in laboratory cultures (Heil, 1986; McKay et al., 2006; Schaeffer et al., 2009; Levandowsky and Kaneta, 1987; Hand et al., 1965; Hunte, 1986; Kamykowski and Mccollum, 1986; Kamykowski et al., 1988, 1992) and from field measurements (Kerfoot et al., 2004; Schofield et al., 2006). Laboratory studies are, however, under controlled environments that may not represent realistic environmental conditions. Additionally, the limited field measurements of vertical migration only documented the behavior of *K. brevis* at one station, and thus are limited in both space and time. On the other hand, while satellite remote sensing provides synoptic and frequent measurements, most ocean color satellites can only observe the subtropical and tropical oceans at most once a day, making it impossible to observe such diurnal changes unless multiple satellites are combined. One possible exception may be the Visible Infrared Imaging Radiometer Suite (VIIRS, 2012 – present), as its wide swath (3060 km) occasionally allows for two observations during a day at a given location in subtropical oceans.

Between July – September 2014, a *K. brevis* bloom occurred in the NE GOM off Florida's Big Bend region, during which several studies documented the bloom size, intensity, and temporal evolution from field and remote sensing observations (Hu et al., 2015; Qi et al., 2015; Elhabashi et al., 2016). The bloom reached a maximum size of about 7000 km^2 by late July, with maximum *K. brevis* concentration of >1 million cells L^{-1}. Field measurements using a glider suggested vertical migration of *K. brevis* inside the bloom (Hu et al., 2016). At a speed of 0.5–1 m h^{-1}, *K. brevis* started to move upward from a depth of 8–10 m around sunrise, and started to move downward from a depth of ~2 m around sunset. Although *K. brevis* vertical migration was observed in the field at synoptic scale (~30 km) in several consecutive days, the glider measurement was still limited in both space and time due to its slow motion (e.g., about 400 m an hour).

* Corresponding author.
 E-mail address: lin.qi@xmu.edu.cn (L. Qi).

Therefore, the objective of this study is to test whether a combination of multiple satellite observations can reveal changes in optical properties of the surface waters in the bloom, from which vertical migration may be inferred. Once confirmed, the findings may be particularly useful for supporting future geo-stationary satellite missions that are designed to "stare" at selected ocean regions multiple times a day, for example from the GEO-CAPE mission recommended by the NRC's decadal survey (Fishman et al., 2012Salisbury et al., 2017).

2. Data and method

Level-2 data from the Moderate Resolution Imaging Spectroradiometer (MODIS) onboard both Terra and Aqua satellites for the bloom period (July - September 2014) were downloaded from NASA Goddard Space Flight Center (http://oceancolor.gsfc.nasa.gov) on 19 April 2016 and mapped to an equidistant cylindrical projection at 1-km spatial resolution. These data contained the standard ocean data products, including spectral remote sensing reflectance (R_{rs}, sr^{-1}) in the visible bands, normalized fluorescence line height (nFLH, mW cm^{-2} μm^{-1} sr^{-1}), surface chlorophyll concentration (Chl, mg m^{-3}), and quality control flags (l2_flags, a 32-bit value for each pixel). Similarly, VIIRS Level-2 data were downloaded from NASA GSFC and also from NOAA STAR CoastWatch from MSL12 processing (ftp://ftp.star.nesdis.noaa.gov/pub/socd1/mecb/coastwatch/viirs/science/L2) about the same time as MODIS download (late April 2016) and mapped to the same equidistant cylindrical projection. The VIIRS data products are similar to those of MODIS, except that nFLH is not available from VIIRS due to its lack of a spectral band around 680 nm. In addition, the particulate backscattering coefficient at 486 nm (b_{bp}486, m^{-1}) and multispectral total absorption coefficients ($a_t(\lambda)$, m^{-1}) were derived from the latest version (version 6; http://www.ioccg.org/groups/Software_OCA/QAA_v6_2014209.pdf) of the Quasi-Analytical Algorithm (QAA) (Lee et al., 2002).

Because of the availability of VIIRS data products from both NASA and NOAA, they were first evaluated to determine which to use in this study. Indeed, although there are slight differences in

the aerosol model look up tables (LUTs) and in the vicarious calibrations between the NASA L2GEN processing and NOAA MSL12 processing, the principles of deriving the Level-2 data products are identical, and their R_{rs} spectra in the green and red bands are very similar. Yet L2GEN R_{rs} spectra shapes in the blue wavelengths appeared to be slightly off for the study region at large viewing angles (not shown here), possibly due to residual errors of polarization correction. Therefore, in this study, VIIRS data from the MSL12 processing were used.

After applying the quality control flags to remove low-quality data, five products were examined: 1) the default blue-green band ratio Chl (OC3, Oreilly et al., 1998), which is available to the user community as a standard data product for both MODIS and VIIRS [note that although recent algorithm updates switched to the hybrid OCI algorithm (Hu et al., 2012), for coastal waters where Chl is >0.25 mg m^{-3} the default algorithm is still OC3]; 2) a new red-green band ratio Chl (RGCI, Le et al., 2013; Qi et al., 2015), which is only available from VIIRS because one of its spectral bands (662–682 nm) partially covers the spectral range of chlorophyll fluorescence; 3) R_{rs} in the visible bands. While the Chl images were used to examine spatial patterns of the bloom, R_{rs} spectra from representative locations outside and inside the bloom were extracted for further analysis and interpretation; 4) b_{bp}486, a measure of particulate concentration in the upper layer; and 5) $a_t(\lambda)$, a measure of absorption in the upper layer.

An ocean glider was deployed from 1 to 16 August 2014 to sample the K. brevis bloom and its surrounding environment. The details of the deployment and its measurements can be found in Hu et al. (2016), where glider data showed vertical migration of phytoplankton in several consecutive days. The upward migration appeared to start around sunrise at a depth of 8–10 m, while the downward migration appeared to start around sunset at a depth of ~2 m. The glider data were binned to image pixel size in Hu et al. (2016), but in this study the glider data were binned in time (every 30 min) and depth (every 1 m) in order to visualize temporal changes. Note that due to cloud cover and measurement logistics glider data were not collected on the same day as the VIIRS measurements examined below.
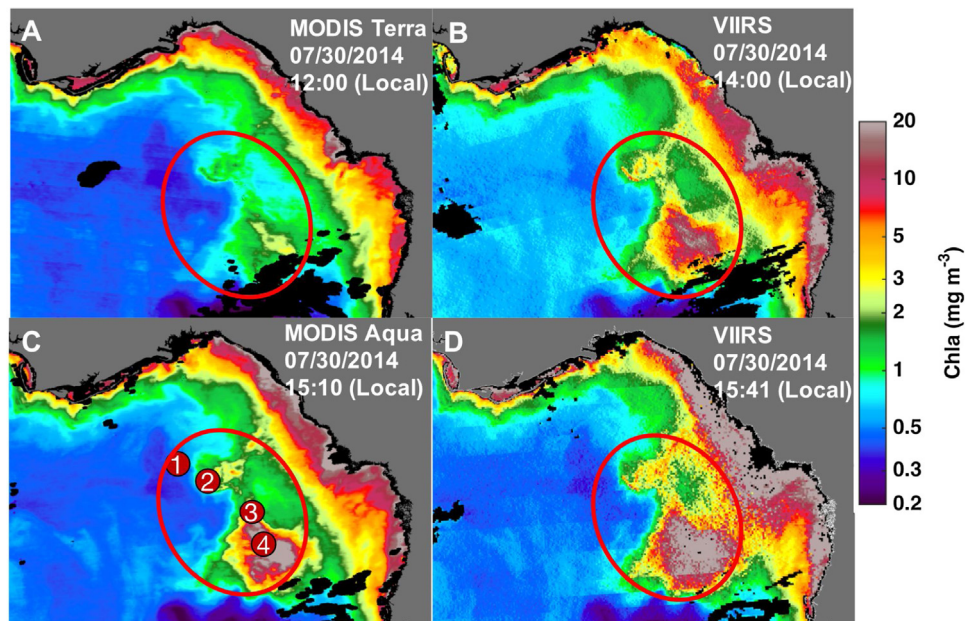
Fig. 1. MODIS and VIIRS OC3 Chl images on 30 July 2014 showing changes in Chl within 3 h 40 min, yet it is believed that some of these observed changes are due to algorithm artifacts and cross-sensor inconsistency. Therefore, they are presented here only to show the bloom's spatial pattern. Four locations (annotated as 1–4) outside and inside the bloom were selected to examine their R_{rs} spectral characteristics.

3. Results

Fig. 1 shows the default MODIS and VIIRS OC3 Chl images on 30 July 2014. In about 3 h 40 min, 4 images were captured: one from MODIS/Terra, one from MODIS/Aqua, and two from VIIRS. All four images showed elevated Chl values along the shorelines, but such elevated values are well known to be a result of algorithm artifact due to shallow bottom, suspended sediments, and interference of colored dissolved organic matter (Cannizzaro et al., 2013). Other than these coastal features, all four images showed the offshore bloom (outlined in red), which was confirmed from field water sampling to be a *K. brevis* bloom (Hu et al., 2015). Within the bloom, it appears that Chl increased with time from the 4 images, yet it would be difficult to draw such conclusions without further analysis because 1) the empirical OC3 Chl is not valid for waters rich in colored dissolved organic matter (CDOM), especially for the Chl range of 0.5–20 mg m^{-3} (Qi et al., 2015); and 2) MODIS and VIIRS were calibrated and processed independently from each other and there may be cross-sensor inconsistency. Indeed, both MODIS sensors are aging (17-years for MODIS/Terra and 15-years for MODIS/Aqua, even though both were designed for 5-year mission life) and have shown signs of degradation in recent years (B. Franz, NASA/GSFC, personal comm.). Spectral analysis and comparison with VIIRS also showed some cross-sensor inconsistency for this bloom event. It is also well known that MODIS/Terra has problems in the blue bands. Therefore, even though MODIS nFLH data products are useful to detect and trace blooms (Hu et al., 2015) and MODIS OC3 Chl data products are also useful to examine offshore bloom patterns in Fig. 1, to observe short-term changes only VIIRS data are presented below.

Fig. 2 shows the VIIRS R_{rs} spectra extracted from 4 representative locations from inside and outside the bloom (Fig. 1C), using data collected from both VIIRS passes. Although the R_{rs} spectra from the two passes appear similar in both spectral shapes and magnitudes for each of the 4 locations, there are indeed observable differences, which might be due to realistic changes in the ocean. To assess this speculation, Chl images from the new RGCI algorithm as well as $b_{bp}486$ and $a_t(\lambda)$ images were generated and examined, and changes in R_{rs} spectral shapes were compared with previously published observations from field measurements.

Fig. 3 shows that within 2 h, the two VIIRS measurements showed different Chl concentrations (A&B) and $b_{bp}486$ (D&E) in the bloom. The difference images in Fig. 3C & F suggest that the Chl difference (15:41 observation minus 14:00 observation) could be 5–10 mg m^{-3} and $b_{bp}486$ difference was close to 0.01 m^{-1}. The RGCI algorithm was tuned and validated using data in the same region (Qi et al., 2015), which showed mean relative error (MRE) of 56% without significant bias. Therefore, such Chl changes from 14:00 to 15:41 exceeded those algorithm uncertainties, which appeared to be realistic. This is also consistent with the much higher $b_{bp}486$ at 15:41. Although the quality of satellite R_{rs} data products (input to the RGCI algorithm) depends on the viewing geometry, the two viewing geometries are similar, with viewing angles of 61° and 65°, respectively, and azimuth angles (relative to the Sun) approaching 90°. Therefore, it is unlikely that such large changes could be explained by changes in geometry or algorithm artifacts in R_{rs}. Instead, these changes may actually be explained by *K. brevis* vertical migration between the two satellite passes, as observable in Fig. 4.

Although the surface Chl derived from the glider measurements are not always higher at 15:41 than at 14:00 (Fig. 4A), the high-Chl layer does appear to be thinner at 15:41 (1 m between 1 and 2 m water depth) than at 14:00 (2 m between 1 and 3 m water depth). Glider data from Day 1 (August 1, Fig. 4B) strongly support the
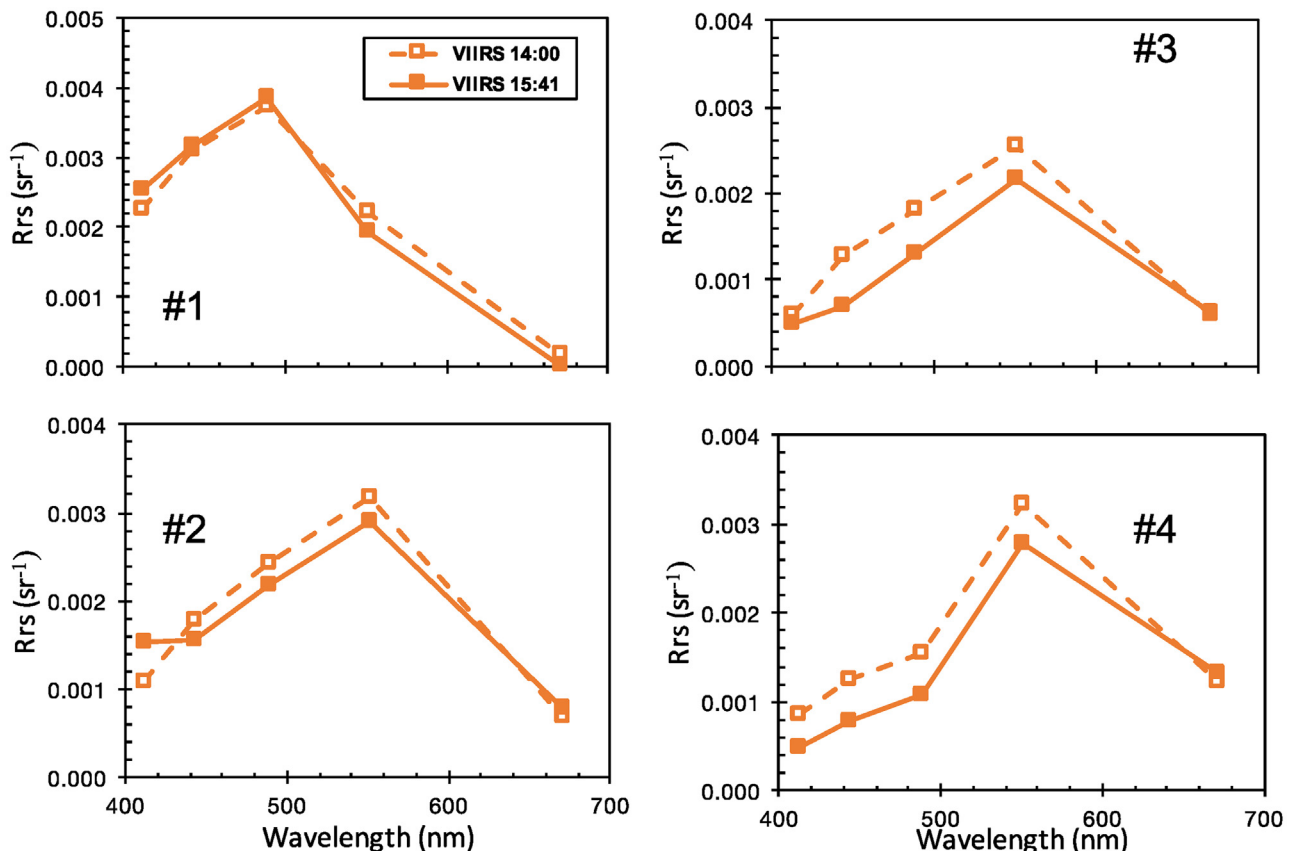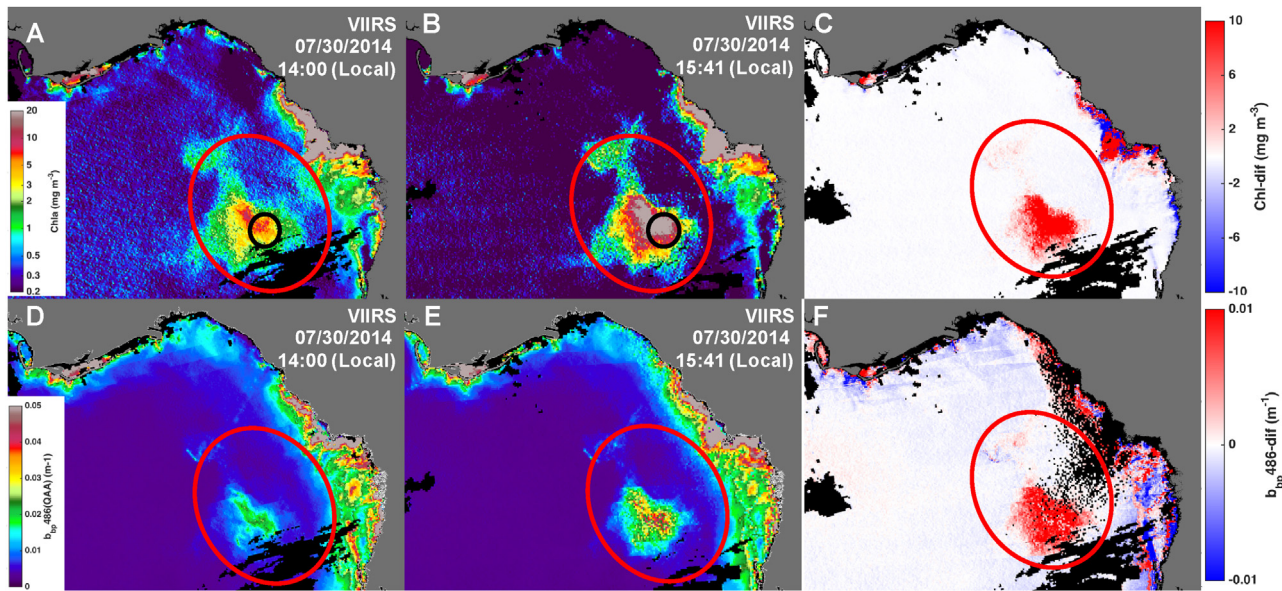

Fig. 2. R_{rs} spectra from the 4 locations (#1–#4, Fig. 1C) from two VIIRS measurements at different times of the same day on 30 July 2014.

Fig. 3. VIIRS RGCI Chl and QAA b_{bp}486 images for two consecutive satellite passes within one day. The pass at 15:41 local time shows higher Chl (B) and b_{bp}486 (E) than the pass at 14:00 local time (A&D), possibly due to vertical migration of *K. brevis*. The images in (C) and (F) show the difference between the two passes. The use of the RGCI algorithm to derive Chl between 0.5 and 20 mg m^{-3} has been demonstrated in Qi et al. (2015). RGCI Chl for relatively clear waters (Chl < 0.5 mg m^{-3}) is not trustable.
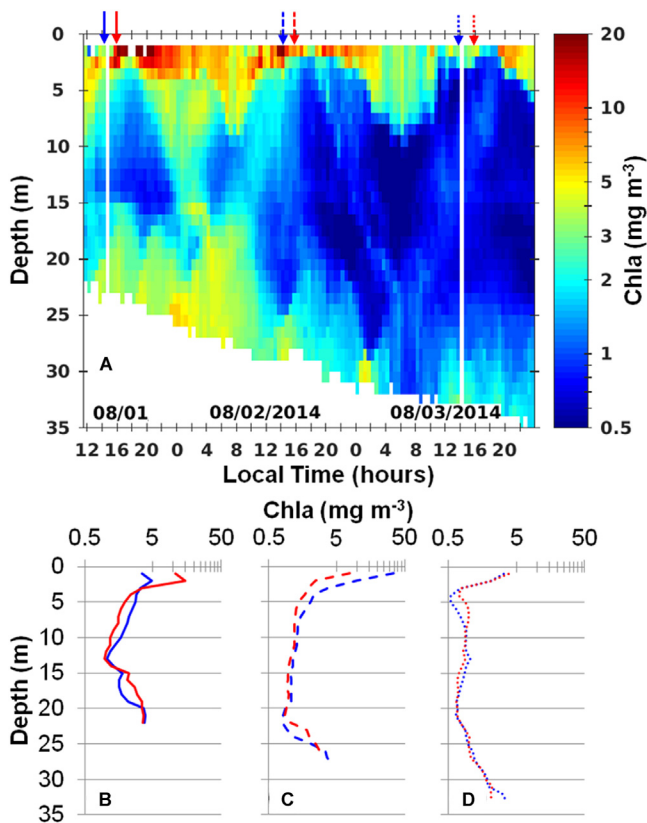

Fig. 4. Glider-measured Chl in between 1 and 4 August 2014 in the same bloom as shown in the VIIRS imagery on 30 July 2014. Data of the top 1 m were discarded due to noise. Data were binned to 30 min in time (corresponding to about 200 m in horizontal distance) and 1 m in vertical distance. (A) blue and red arrows annotate local time 14:00 and 15:41, respectively, corresponding to the two VIIRS passes on a different day; (B)–(D) Chl vertical profiles for the two times on 1, 2, and 3 August, respectively. (For interpretation of the references to colour in this figure legend, the reader is referred to the web version of this article.)

hypothesis of upward migration from 14:00 to 15:41 as the surface layer between 1 and 3 m showed much higher (~5–10 mg m^{-3}) Chl at 15:41 than at 14:00, while the deeper layer between 5 and 10 m showed reversed pattern (i.e., lower Chl at 15:41 than at 14:00). In contrast, Days 2 and 3 on August 2–3 (Fig. 4C-D) did not show significant changes in the deep layer, therefore the changes in the surface layer may originate from horizontal changes rather than vertical changes. Indeed, *K. brevis* is known to be very patchy where concentration can change significantly in hundreds or tens of meters (Tomlinson et al., 2004). Such small-scale changes cannot be captured by VIIRS (750-m pixels) but can be captured by gliders, even after the ~200-m horizontal binning in Fig. 4. Therefore, while Day 1 profiles strongly support the hypothesis of upward migration from 14:00 to 15:41, Days 2 and 3 could have alternative explanations. Note that Day 1 (August 1) is also closer to the VIIRS observations (July 30) than Days 2 and 3.

The hypothesis that the changes in VIIRS-derived Chl might be a result of *K. brevis* vertical migration is further supported by the spectral analysis of the bloom waters. Fig. 5A shows that R_{rs} from a location inside the bloom (marked as a black circle in Fig. 3) changed between the two satellite passes. The changes in their spectral shapes can be clearly observed in the normalized R_{rs} spectra in Fig. 5B. Such a change agrees nicely with previously published results from repeated measurements at another location on the west Florida Shelf (Fig. 5C & D of Schofield et al., 2006). In the normalized spectra, the 672-nm band showed higher R_{rs} in late afternoon than in earlier measurements from both VIIRS and field measurements, and the curvature at 443 and 488 nm (relative to 412 and 551 nm) also became more apparent in late afternoon (dotted circles). Although most curvature changes occurred around 480 nm in Fig. 5D but around 443 nm in Fig. 5C, the changes in the overall spectral shapes agree with each other, especially for the red band that suffers less from atmospheric correction residual errors. Additionally, the QAA-derived $a_t(\lambda)$ coefficients also increased from 14:00 to 15:41 (Fig. 5A empty symbols).

In summary, the agreement between VIIRS and field measurements in the spectral shape changes in addition to the RGCI Chl and QAA b_{bp}486 changes and the findings from the glider measurements in the same bloom at a later time all support the hypothesis that the VIIRS observed surface changes are possibly due to *K.*
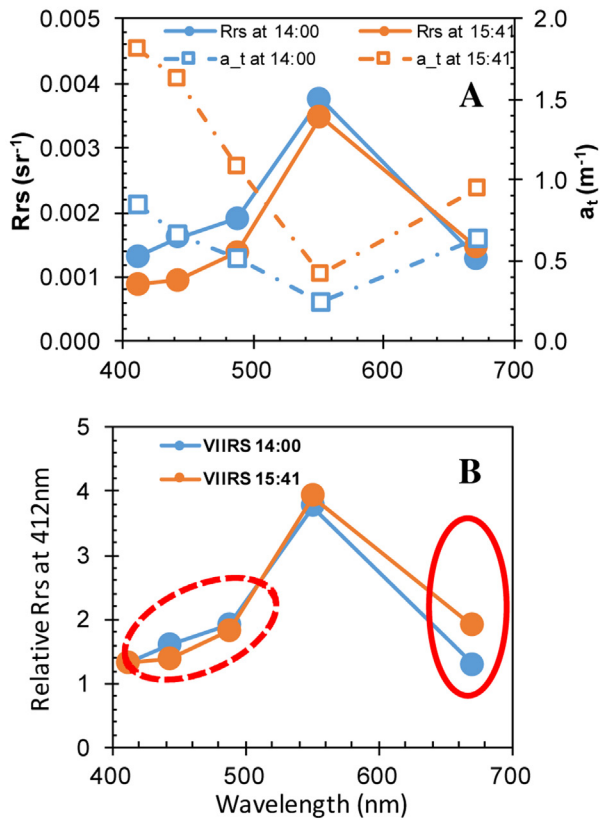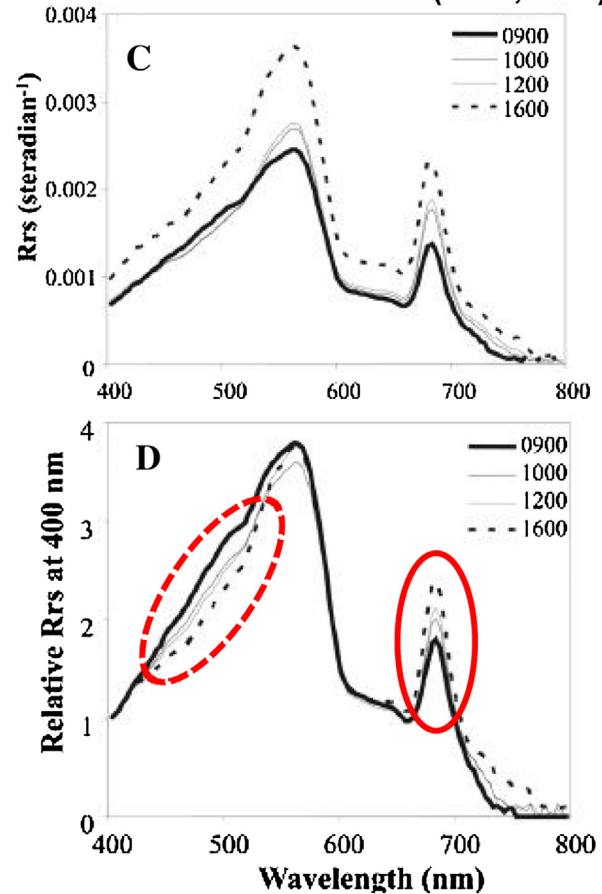
Fig.5. (A) and (B): VIIRS R_{rs} spectra (raw and normalized at 412 nm) from a location inside a *K. brevis* bloom (marked by "+" in Fig. 3) collected at 14:00 and 15:41 local time on 30 July 2014. Also plotted in (A) are the corresponding total absorption coefficients (a_t, m^{-1}, empty symbols) derived from the R_{rs} spectra using the QAA algorithm; (C) and (D) R_{rs} spectra from repeated measurements over a *K. brevis* bloom site (Schofield et al., 2006) showing changes between morning measurements (0900–1200, local time 9:00–12:00) and afternoon measurement (1600, local time 16:00). Note that the changes in spectral curvature around 443 and 488 nm as well as around 670 nm are consistent between VIIRS and field measurements (outlined in dotted and solid circles, respectively). (C) and (D) are reproduced from Schofield et al. (2006) with publisher's permission.
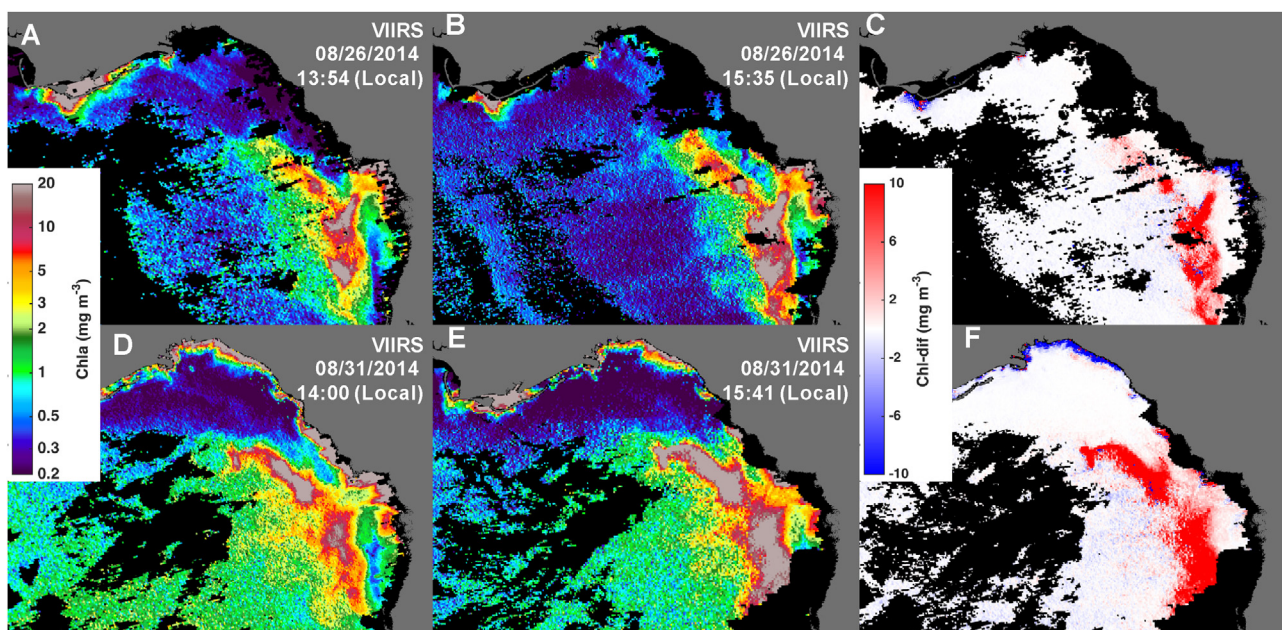
Fig. 6. Two other cases showing RGCI Chl increases between two VIIRS passes in the same day. Top: 26 August 2014; Bottom: 31 August 2014. The right-most column shows the difference images.

brevis vertical migration, although other possibilities (e.g., algorithm artifacts) cannot be completely ruled out. However, during the 3-month bloom, two other instances of bi-daily VIIRS measurements with minimal cloud cover and minimal sun glint contamination were available, and both showed similar results (Fig. 6). On both 26 and 31 August 2014, the later VIIRS images always showed higher RGCI Chl than the earlier images in the same days, suggesting that the observation of diurnal changes could be generalized for this bloom.

4. Discussion

4.1. Realistic or artifacts?

While for several decades satellite data have been used to examine temporal changes, most studies focused on changes on a statistical level (e.g., monthly mean, regional mean) rather than on changes from individual images as shown here. This is because, statistically, the many uncertainties in satellite data can be averaged out in spatial and/or temporal means. This is exactly why the analyses of RGCI Chl and R_{rs} spectral shapes were used to verify whether the observed changes over the known *K. brevis* bloom were realistic or due to sensor/algorithm artifacts. From several lines of supporting data (changes in spectral shapes, and *K. brevis* vertical migration from the glider measurement in the same bloom), one may argue that the observed changes in the RGCI Chl could be realistic, especially after the fact that such changes exceeded the RGCI Chl uncertainties (Qi et al., 2015).

One interesting question is whether such observed changes can be used to infer *K. brevis* vertical migration unambiguously, as other processes such as physical aggregation may cause similar changes. In this case, because the bloom size appeared to be stable but the intensity changed between the two VIIRS images (Fig. 3), physical aggregation may be ruled out as a possible cause. *K. brevis* is known to have a low reproduction rate (0.2–1.0 divisions per day, Steidinger et al., 1998), therefore the intense changes in both Chl and $b_{bp}486$ within 2 h could not be explained by *K. brevis* reproduction either. Changes in vertical distributions appeared to be the only plausible explanation as long as the VIIRS-observed changes are realistic instead of algorithm/calibration artifacts. This is true even without the glider measurements to support such an inference.

Although the glider measurements did not directly prove the hypothesis of upward migration from 14:00 to 15:41 because the glider data were collected on different days from the VIIRS measurements and due to possible *K. brevis* patchiness with the top layer, they did support such a hypothesis because Day 1 (August 1) showed strong evidence of vertical migration. Data from Days 2 and 3, however, could have alternative explanations. Furthermore, from the data presented in Hu et al. (2016), there is no reason to believe that *K. brevis* upward migration stopped during 14:00–15:41 (downward movement began around sunset). In any case, given the limited observations from this single event, more studies for other bloom cases, especially from other regions around the world, are required to further confirm whether such an inference can be generalized.

4.2. Support for geostationary observations

While multiple polar-orbiting sensors may provide more than one observation a day for the GOM, interpretation of the observed changes is very difficult, especially when most polar-orbiting sensors are designed to take measurements around local solar noon (typically within 2–3 h). Even though after significant amount of community effort in cross-sensor calibration and data product validation the MODIS and VIIRS data products appeared to be overall consistent on a statistical level (Hlaing et al., 2013; Hu and Le, 2014; Barnes and Hu, 2015, 2016), interpreting changes within 2–3 h from two or three sensors is still difficult because of differences in sensor design and calibration as well as their response to input signal at different observing geometry.

The case study here demonstrates the value of using a single sensor to observe short-term changes, which strongly supports geostationary ocean color missions, for example the GEO-CAPE mission currently being under design and planned by NASA (Fishman et al., 2012; Salisbury et al., 2017). Indeed, with 8 hourly measurements per day, the proof-of-concept Geostationary Ocean Color Imager (GOCI, 2010–present) has already shown advantage over polar-orbiters in capturing short-term changes of algal blooms and water quality in coastal waters around South Korea, East China Sea, and the Yellow Sea (Choi et al., 2012, 2014; He et al., 2013; Lou and Hu, 2014; Son et al., 2012; Wang et al., 2013). Observations from geostationary sensors designed not for ocean color have also been shown useful in detecting diurnal changes of water properties, although due to the low signal-to-noise ratios they could only be used to observe bright targets such as waters rich in sediments (Neukermans et al., 2012) or covered by floating mats of algae (Hu and Feng, 2014). The case study here showed the value of VIIRS (two overpasses within 2 h for the study region every 4–5 days), particularly when combined with field observations, in capturing short-term changes of the surface ocean. Different from previous studies using VIIRS (Arnone et al., 2016), such short-term changes appeared to be linked to vertical changes of *K. brevis*. Because *K. brevis* moves faster immediately after sunrise and sunset than at other times of a day (Hu et al., 2016), the availability of a future geostationary ocean color sensor to measure the ocean from early morning to late afternoon is expected to significantly enhance our capacity to observe similar short-term changes that are related to bloom dynamics. Nevertheless, the challenges in using such geostationary sensors to quantify diurnal changes still need to be addressed (Ruddick et al., 2014).

5. Conclusion

With the support of glider measurements and after extensive data analysis, it is shown that VIIRS is able to capture changes of surface reflectance, chlorophyll concentration, water column absorption, and particulate backscattering in a *K. brevis* bloom within 2 h, which were inferred to be a result of *K. brevis* vertical migration. Such a capacity is the result of tremendous community efforts in calibrating the sensor and improving the atmospheric correction and bio-optical inversion algorithms. On the other hand, the findings here also strongly support similar observations from a geostationary platform in the future to observe short-term dynamics of phytoplankton blooms.

References

Arnone, R., Vandermeulen, R.A., Ladner, S., Ondrusek, M., Kovach, C., Yang, H., Salisbury, J., 2016. Diurnal changes in ocean color in coastal waters. Proc. SPIE 9827, Ocean Sensing and Monitoring VIII, 982711 (May 17) doi:http://dx.doi.org/10.1117/12.2241018.

Barnes, B.B., Hu, C., 2015. Cross-sensor continuity of satellite-derived water clarity in the Gulf of Mexico: insights into temporal aliasing and implications for long-term water clarity assessment. IEEE Trans. Geosci. Remote Sens. 53, 1761–1772.

Barnes, B.B., Hu, C., 2016. Dependence of satellite ocean color data products on viewing angles: a comparison between SeaWiFS, MODIS, and VIIRS. Remote Sens. Environ. 175, 120–129.

Cannizzaro, J., Hu, C., Carder, K.L., Kelble, C.R., Melo, N., Johns, E.M., Vargo, G.A., Heil, C.A., 2013. On the accuracy of SeaWiFS ocean color data products on the West Florida Shelf. J. Coast. Res. 29 (6), 1257–1272. doi:http://dx.doi.org/10.2112/JCOASTRES-D-12-00223.1.

Choi, J.-K., Park, Y.J., Ahn, J.H., Lim, H.-S., Eom, J., Ryu, J.-H., 2012. GOCI, the world's first geostationary ocean color observation satellite, for the monitoring of temporal variability in coastal water turbidity. J. Geophys. Res. 117, 9004.

Choi, J.-K., Min, J.-E., Noh, J.-H., Park, J.-H., 2014. Harmful algal bloom (HAB) in the east sea identified by the geostationary ocean color imager (GOCI). Harmful Algae 39, 295–302.

Elhabashi, A., Ioannou, I., Tomlinson, M.C., Stumpf, R.P., Ahmed, S., 2016. Satellite retrievals of Karenia brevis harmful algal blooms in the West Florida shelf using neural networks and comparisons with other techniques. Remote Sens. 8 (5) .

Fishman, J., Iraci, L.T., Al-Saadi, J., et al., 2012. The United States' next generation of atmospheric composition and coastal ecosystem measurements: NASA's Geostationary Coastal and Air Pollution Events (GEO-CAPE) mission. Bull. Am. Meteor. Soc. 93, 1547–1566. doi:http://dx.doi.org/10.1175/BAMS-D-11-00201.1.

Hand, W.G., Collard, P.A., Davenport, D., 1965. The effects of temperature and salinity change on swimming rate in the dinoflagellates. Gonyaulax Gyrodinium. Biol. Bull. 128, 90–101.

He, X., Bai, Y., Pan, D., Huang, N., Dong, X., Chen, J., Chen, C.-T.A., Cui, Q., 2013. Using geostationary satellite ocean color data to map the diurnal dynamics of suspended particulate matter in coastal waters. Remote Sens. Environ. 133, 225–239.

Heil, C., 1986. Vertical Migration of Ptychodiscus Breve (Davis). M.S. Thesis. University of South Florida.

Hlaing, S., Harmel, T., Gilerson, A., Arnone, R., 2013. Evaluation of the VIIRS ocean color monitoring performance in coastal regions. Remote Sen. Environ. 139, 398–414.

Hu, C., Feng, L., 2014. GOES Imager shows diurnal change of a Trichodesmium erythraeum bloom on the west Florida shelf. IEEE Geosci. Remote Sens. Lett. 11, 1428–1432.

Hu, C., Le, C., 2014. Ocean color continuity from VIIRS measurements over Tampa Bay. IEEE Geosci. Remote Sens. Lett. 11, 945–949. doi:http://dx.doi.org/10.1109/LGRS.2013.2282599.

Hu, C., Lee, Z., Franz, B., 2012. Chlorophyll algorithms for oligotrophic oceans: a novel approach based on three-band reflectance difference. J. Geophys. Res. 117 (C01011) doi:http://dx.doi.org/10.1029/2011JC007395.

Hu, C., Barnes, B.B., Qi, L., Corcoran, A.A., 2015. A harmful algal bloom of Karenia brevis in the northeastern Gulf of Mexico as revealed by MODIS and VIIRS: a comparison. Sensors 15, 2873–2887. doi:http://dx.doi.org/10.3390/s150202873.

Hu, C., Barnes, B.B., Qi, L., Lembke, C., English, D., 2016. Vertical migration of Karenia brevis in the northeastern Gulf of Mexico observed from glider measurements. Harmful Algae 58, 59–65. doi:http://dx.doi.org/10.1016/j.hal.2016.07.005.

Hunte, W., 1986. Effects of temperature on swimming speed of the dinoflagellate Gymnodinium splendens. Fish. Bull. 84, 460–463.

Kamykowski, D., Mccollum, S.A., 1986. The temperature acclimated swimming speed of selected marine dinoflagellates. J. Plankton Res. 8 (2), 275–287.

Kamykowski, D., Mccollum, S.A., Kirkpatrick, G., 1988. Observations and a model concerning the translational velocity of a photosynthetic marine dinoflagellate under variable environmental conditions. Limnol. Oceanogr. 33 (1), 66–78.

Kamykowski, D., Reed, R.E., Kirkpatrick, G.J., 1992. Comparison of sinking velocity, swimming velocity, rotation and path characteristics among six marine dinoflagellate species. Mar. Biol. 113, 319–328.

Kerfoot, J., Kirkpatrick, S., Lohrenz, S., Mahoney, K., Moline, M., Schofield, O., 2004. Harmful Algae 2002. In: Steidinger, K.A., Landsberg, J.H., Tomas, C.R., Vargo, G.A. (Eds.), Florida Fish and Wildlife Conservation Commission, Florida Institute of Oceanography, and Intergovernmental Oceanographic Commission of UNESCO P 279–281.

Le, C., Hu, C., Cannizzaro, J., English, D., Kovach, C., 2013. Climate-driven chlorophyll a changes in a turbid estuary: observation from satellites and implications for management. Remote Sens. Environ. 130, 11–24.

Lee, Z., Carder, K.L., Arnone, R., 2002. Deriving inherent optical properties from water color: a multiband quasi analytical algorithm for optically deep waters. Appl. Opt. 41 (27), 5755–5772.

Levandowsky, M., Kaneta, P., 1987. Behaviour in dinoflagellates. In: Taylor, F.J.R. (Ed.), The Biology of Dinoflagellates. Blackwell Scientific Publications, Oxford, pp. 360–398.

Lou, X., Hu, C., 2014. Diurnal changes of a harmful algal bloom in the East China Sea: observations from GOCI. Remote Sens. Environ. 140, 562–572.

McKay, L., Kamykowski, D., Milligan, E., Schaeffer, B., Sinclair, G., 2006. Comparison of swimming speed and photophysiological responses to different external conditions among three Karenia brevis strains. Harmful Algae 5, 623–636.

Neukermans, G., Ruddick, K.G., Greenwood, N., 2012. Diurnal variability of turbidity and light attenuation in the southern North Sea from the SEVIRI geostationary sensor. Remote Sens. Environ. 124, 564–580. doi:http://dx.doi.org/10.1016/j.rse.2012.06.003.

Oreilly, J.E., Maritorena, S., Mitchell, B.G., Siegel, D.A., Carder, K.L., Garver, S.A., Mcclain, C.R., 1998. Ocean color chlorophyll algorithm for SeaWiFS. J. Geophys. Res. 24937–24953.

Qi, L., Hu, C., Cannizzaro, J.P., Corcoran, A.A., English, D., Le, C., 2015. VIIRS observations of a Karenia brevis bloom in the Northeastern Gulf of Mexico in the absence of a fluorescence band. IEEE Geosci. Remote Sens. Lett. 12 (11), 2213–2217.

Ruddick, K., Neukermans, G., Vanhellemont, Q., Jolivet, D., 2014. Challenges and opportunities for geostationary ocean colour remote sensing of regional seas: a review of recent results. Remote Sens. Environ. 146, 63–76.

Salisbury, J., Davis, C., Erb, A., Hu, C., Gatebe, C., Jordan, C., Lee, Z., Mannino, A., Mouw, C.B., Schaaf, C., Schaeffer, B.A., Tzortziou, M., 2017. Coastal observations from a new vantage point. EOS 98 (1), 20–25. doi:http://dx.doi.org/10.1029/2016EO062707.

Schaeffer, B.A., Kamykowski, D., Sinclair, G., McKay, L., Milligan, E.J., 2009. Diel vertical migration thresholds of Karenia brevis (Dinophyceae). Harmful Algae 8, 692–698.

Schofield, O., Kerfoot, J., Mahoney, K., Moline, M., Oliver, M., Lohrenz, S., Kirkpatrick, G., 2006. Vertical migration of the toxic dinoflagellate Karenia brevis and the impact on ocean optical properties. J. Geophys. Res. 111, C06009. doi:http://dx.doi.org/10.1029/2005JC003115.

Son, Y.B., Min, J.-E., Ryu, J.-H., 2012. Detecting massive green algae (Ulva prolifera) blooms in the yellow sea and East China sea using geostationary ocean color imager (GOCI) data. Ocean Sci. J. 47 (3), 359–375.

Steidinger, K.A., Vargo, G.A., Tester, P.A., Tomas, C.R., et al., 1998. Bloom dynamics and physiology of Gymnodinium breve with emphasis on the Gulf of Mexico. In: Anderson, D.M. (Ed.), Physiological Ecology of Harmful Algal Blooms. Springer Verlag, Berlin/Heidelberg, pp. 133–153.

Tomlinson, M.C., Stumpf, R.P., Ransibrahmanakul, V., Truby, E.W., Kirkpatrick, G.J., Pederson, B.A., Vargo, G.A., Heil, C.A., 2004. Evaluation of the use of SeaWiFS imagery for detecting Karenia brevis harmful algal blooms in the eastern Gulf of Mexico. Remote Sens. Environ. 91 (3–4), 293–303.

Wang, M., Ahn, J.-H., Jiang, L., Shi, W., Son, S.-H., Park, Y.-J., Ryu, J.-H., 2013. Ocean color products from the Korean geostationary ocean color imager (GOCI). Opt. Express 21 (3), 3835–3849.